Available online at www.sciencedirect.com
SCIENCE DIRECT®
Polyhedron 22 (2003) 3277–3288
POLYHEDRON
www.elsevier.com/locate/poly

# Further studies of [ω-(haloalkylstannyl)alkyl]phosphine oxides. Structures of bis[2-(bromodimethylstannyl)ethyl]phenylphosphine oxide and *t*-butyl[3-(iododimethylstannyl)propyl]phenylphosphine oxide

William T.A. Harrison [a], R. Alan Howie [a,*], Marcel Jaspars [a], Solange M.S.V. Wardell [b], James L. Wardell [c]

[a] *Department of Chemistry, University of Aberdeen, Meston Walk, Old Aberdeen AB24 3UE, UK*
[b] *Departamento de Química Inorgânica, Instituto de Química, Universidade Federal Fluminense, 24020-150 Niterói, RJ, Brazil*
[c] *Departamento de Química Inorgânica, Instituto de Química, Universidade Federal do Rio de Janeiro, 21945-970 Rio de Janeiro, RJ, Brazil*

Received 11 June 2003; accepted 21 July 2003

**Abstract**

The crystal structures of bis[2-(bromodimethylstannyl)ethyl]phenylphosphine oxide **3** (X = Br), and *t*-butyl[3-(iododimethylstannyl)propyl]phenylphosphine oxide **7** (X = I), have been determined. Compound **7** (X = I), grown from EtOH solution, is a chelated complex as a consequence of an intramolecular Sn–O interaction and hence contrasts with the previously reported [3-(iododimethylstannyl)propyl]diphenylphosphine oxide, grown from alcohol media solution, which has an intermolecular Sn–O linked chain structure. Molecules of **7** (X = I) are linked into double chains via C–H–I and C–H–π interactions. Compound **3** (X = Br), isostructural with previously reported **3** (X = Cl) obtained from $CH_2Cl_2$ solution, contains two distinct trigonal bipyramidal tin centres. One Sn centre is intramolecularly bound to the O, i.e., one $PhP(O)CH_2CH_2$ fragment is acting as a C,O-chelating unit, while the other Sn centre is weakly bonded to a Br ligand from another molecule to set up zig zag chains of molecules. Intermolecular interactions, C–H–Br and C–H–π, create a double layer of molecules. Detailed $^1$H NMR spectra of **3** are reported.


*Keywords:* Organotin; Phosphine oxide; Crystal structures; Chelation

## 1. Introduction

Structures of ω-(stannylalkyl)phosphine oxides, e.g., $X_nR_{3-n}Sn(CH_2)_mP(O)R'R''$, (R and R′ = alkyl or aryl; R″ = alkyl, aryl or alkoxy; $m = 2$ [1–6] or 3 [3,7]) and $[X_nR_{3-n}Sn(CH_2)_2]_2P(O)R'$ (X = halide; R, R′ and R″ = alkyl or aryl; $n = 0$ or 1 [8]), have been variously studied. While in non-halogenated compounds, such as $R_3Sn(CH_2)_mP(O)R'R''$ and $[R_3Sn(CH_2)_2]_2P(O)R'$ (R and R′ = alkyl or aryl; R″ = alkyl, aryl or alkoxy; $m = 2$ or 3) tin is invariably four coordinate both in solution and in the solid state at least five coordination occurs in the halide derivatives in both phases.

As shown recently [6], $XMe_2SnCH_2CH_2P(O)Ph_2$ **1** (X = Cl, Br or I), crystallises in two distinct unsolvated forms, a polymeric, zig zag chain form, with intermolecular Sn–O bonds, *polymer*-**1**, in which $CH_2CH_2P(O)Ph_2$ acts as a bridging ligand, and a molecular form, *chelate*-**1** [6], with intramolecular Sn–O bonds and the $CH_2CH_2P(O)Ph_2$ moiety chelating with the formation of a five-membered ring. The tin centres in both forms have trigonal bipyramidal geometries with O and the X group in axial positions, see Figs. 1a and b. The polymeric forms were isolated on recrystallisation from alcohols, e.g., MeOH and EtOH, and the chelate forms from non-hydroxylic solvents, such as $Me_2CO$ and chlorocarbons. In contrast to **1** (X = Cl, Br or I) **1**

* Corresponding author. Tel.: +44-1224-272907; fax: +44-1224-272921.
*E-mail address:* r.a.howie@abdn.ac.uk (R.A. Howie).

0277-5387/$ - see front matter © 2003 Elsevier Ltd. All rights reserved.
doi:10.1016/S0277-5387(03)00470-4

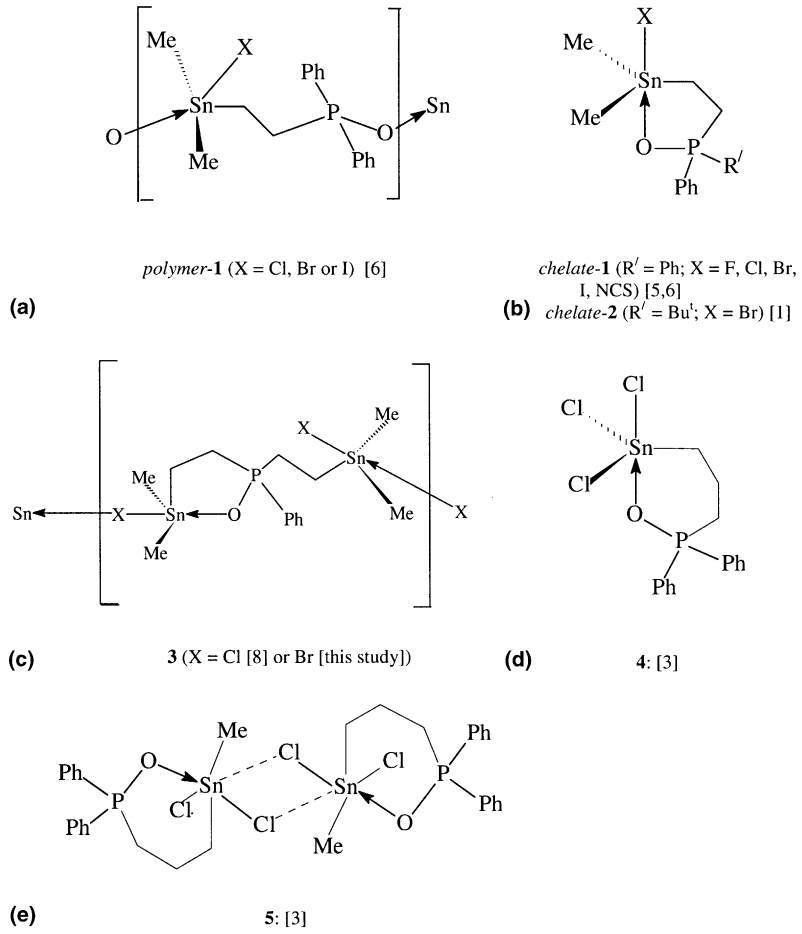


Fig. 1. Solid state arrangements, ignoring H-bonds and other intermolecular interactions, for **1**–**5.**

(X = NCS) recrystallised in the chelate form in all solvents used [6]. Chelate forms of $BrMe_2SnCH_2CH_2P(O)PhBu^t$ **2** [1] and **1** (X = F), [5], both recrystallised from $CH_2Cl_2$/hexane [3], had been previously reported. The differences in the effects of the solvents used for recrystallisation are linked to the different H-bonding abilities of the solvents, see later.

The solid-state structure of bis[2-(chlorodimethylstannyl)ethyl]phosphine oxide, $(XMe_2SnCH_2CH_2)_2P(O)Ph$ **3** (X = Cl), recrystallised from $CH_2Cl_2$/hexane, has been reported by Weichman and co-workers [8]. Both tin centres in solid **3** (X = Cl) are 5-co-ordinate, but with distinct trigonal bipyramidal geometries. One Sn centre is intramolecularly bound to the O, i.e., one $PhP(O)CH_2CH_2$ fragment is acting as a C,O-chelating unit, while the other Sn centre is weakly bonded to a Cl ligand from another molecule, which thus results in halide bridged chains of molecules, see Fig. 1c. The most electronegative atoms occupy the axial sites at both tin centers in **3**.

Crystal structures of samples of $Cl_3SnCH_2CH_2CH_2P(O)Ph_2$ **4** and $Cl_2MeSnCH_2CH_2CH_2P(O)Ph_2$ **5**, recrystallised from $CH_2Cl_2$/hexane, were recently reported by Seibert et al. [3]. In both compounds, the $CH_2CH_2CH_2P(O)Ph_2$ ligands form six-membered chelate rings, but whereas **4** was reported to be a molecular species with a 5-coordinate Sn centre, see Fig. 1d, compound **5** exists as a dimeric compound with 6-coordinate Sn, due to additional, albeit weak, Sn–Cl bridging, see Fig. 1e. Limited solid-state structural parameters for the other member of the $Cl_{3-n}Me_nSnCH_2CH_2CH_2P(O)Ph_2$ series ($n = 0$ to 2), namely $XMe_2SnCH_2CH_2CH_2P(O)Ph_2$ **6** (X = Cl) were cited in Mitchell and Godry's paper in 1996 [7,9], but the full details have remained unpublished. Compound **6** (X = Cl) is apparently a chelated complex, but the precise geometry, the molecularity and solvent of crystallisation of the sample of **6** (X = Cl) used in the determination are unknown.

It is apparent for all the ω-(haloalkylstannylalkyl)phosphine oxides, **1**–**6**, that while Sn–O interactions generally occur, subtle structural differences can arise depending on, among other factors, the solvent used for recrystallisation. To investigate further the effects of recrystallisation media, the structures of **3** (X = Br) and $XMe_2SnCH_2CH_2CH_2P(O)PhBu^t$ **7** (X = I),

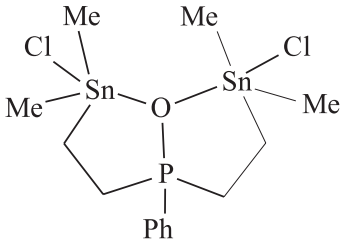


Fig. 2. Monomeric structure in solution proposed for **3** (X = Cl) [8].

both recrystallised from ethanol, have been determined and are reported.

IR and multinuclear NMR spectra clearly show that Sn–O interactions in ω-(haloalkylstannylalkyl)phosphine oxides also occur in solution, at least, that is, in non-coordinating solvents [1–4,6,7]. However differences between solid state and solution structures may arise. For example, Weichmann and co-workers [8] reported that both Sn groups in $(XMe_2SnCH_2CH_2)_2P(O)Ph$ **3** in chloroform solutions appeared to be intramolecularly coordinated to O in a symmetric fashion from $^{119}Sn$ NMR spectral data, see Fig. 2. We have investigated further the $^1H$ NMR spectra of **3** (X = Cl, Br and I) and report the details here.

## 2. Results and discussion

### 2.1. Synthesis

Halide exchange reactions of **3** (X = Cl) using NaBr or NaI in acetone gave **3** (X = Br or I). Elemental analysis and NMR spectra indicated that complete exchange had occurred for the samples used. Suitable crystals of **3** (X = Br) for X-ray crystallography were obtained from $CH_2Cl_2$/hexane solutions or were grown by slow evaporation of EtOH solutions. Compound **7** (X = I) was obtained from the reaction of $Me_3SnCH_2CH_2CH_2PPhBu^t$ [10] and iodine [1:1 mole ratio] in $CHCl_3$ in a vessel open to the air. As shown by the X-ray structure determination the sample of **7** (X = I) obtained by recrystallisation of the solid reaction product from EtOH contained ca. 3.7% of the diiodide, $I_2MeSnCH_2CH_2CH_2P(O)PhBu^t$ **8**, formed by further iodo-demethylation of **7** (X = I).

### 2.2. Crystal structure of 3 (X = Br)

Samples of crystalline **3** (X = Br), obtained either from EtOH or $CH_2Cl_2$/hexane solutions, were shown to have the same solid-state structure, which was isostructural with **3** (X = Cl), obtained from $CH_2Cl_2$/hexane solution [8]. The lack of specific solvent influences on the crystal structure of the bistannylated-phosphine oxide **3** (X = Br), contrasts with the situation found for the monostannylated-phosphine oxides **1** (X = Cl, Br and I) [6]. The data set discussed here was obtained from the crystals grown from EtOH solution.

As a consequence of the two distinct 5-coordinate, trigonal bipyramidal, tin centres, there are three different Sn–Br bond lengths in **3** (X = Br) – intramolecular Sn1–Br1 [2.6918(8) Å], intramolecular Sn2–Br2 [2.5367(9) Å] and intermolecular and bridging, Sn2–Br1$^i$ [3.5826(9) Å], see Fig. 3 and Table 1: symmetry operation (i) $1-x,\ y-1/2,\ 1/2-z$. The intramolecular Sn2–Br2 bond length is essentially the same as the sum of the covalent bond radii, 2.54 Å, [11] for Sn and Br, while the other two distinct Sn–Br bond lengths are well within the sum of the van der Waals radii, 4.15 Å, [11]. The bridging Sn2–Br1$^i$ bond is clearly weak, but its effect on the other bond angles at Sn2 is clear. The chelated tin centre, Sn1, due mainly to the chelate bite angle, O1–Sn1–C3 = 80.70(18)°, has a distorted trigonal bipyramidal geometry for which $\tau$ parameter calculation indicates 79% trigonal bipyramidal and 21% square pyramidal contributions to the overall geometry [12]. The axial sites are occupied by O1 and Br1, with O1–Sn1–Br1 = 172.10(9)°. The chelate ring has a twist conformation about C3–C4 as shown by the pucker parameters, $Q = 0.462(5)$ Å and $\phi = 307.4(6)°$ [13]. The bond angles and lengths pertaining to the chelated tin centres in **3** (X = Br) and in **1** (X = Br) are very similar, see Table 2. The slightly longer Sn–Br and the shorter Sn–O bond in **1** (X = Br), however, indicate that the Sn–O intramolecular interaction in this compound is just the stronger. Data are also listed in Table 2 for related compounds.

The geometry at the non-chelated tin centre, Sn2 in **3** (X = Br) is also distorted trigonal bipyramidal with the axial positions occupied by Br2 and the bridging Br1$^i$ and *trans* axial angle Br1$^i$–Sn2–Br2 = 169.50(3)°. The bridging Sn2–Br1$^i$ bonds set up zig zag primary chains

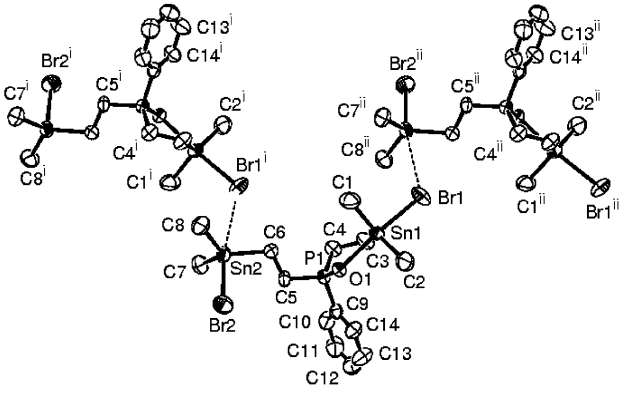


Fig. 3. A portion of a chain of molecules of **3** (X = Br) propagated in the direction of *b* by the operation of a crystallographic 2-fold screw axis. Non-H atoms are shown as 50% ellipsoids and H atoms have been omitted for clarity. Dashed lines represent intermolecular Sn2–Br1 contacts. Symmetry operations: (i), $1-x,\ y-1/2,\ 1/2-z$; (ii), $1-x,\ y+1/2,\ 1/2-z$.

Table 1
Selected geometric parameters, (Å, °) for **3** (X = Br)

| | | | |
|---|---|---|---|
| Sn1–Br1 | 2.6918(8) | Sn2–Br2 | 2.5367(9) |
| Sn1–O1 | 2.354(3) | Sn2–Br1$^{i}$ | 3.5826(9) |
| Sn1–C1 | 2.120(7) | Sn2–C6 | 2.152(6) |
| Sn1–C2 | 2.096(7) | Sn2–C7 | 2.135(7) |
| Sn1–C3 | 2.154(6) | Sn2–C8 | 2.120(7) |
| C3–C4 | 1.530(8) | C6–C5 | 1.516(8) |
| C4–P1 | 1.803(5) | C5–P1 | 1.801(5) |
| P1–O1 | 1.518(4) | P1–C9 | 1.794(6) |
| Br1–Sn–O1 | 172.10(9) | Br1$^{i}$–Sn2–Br2 | 169.50(3) |
| Br1–Sn1–C1 | 96.4(2) | Br2–Sn2–C6 | 97.28(16) |
| O1–Sn1–C1 | 90.3(2) | Br1$^{i}$–Sn2–C6 | 72.43(16) |
| Br1–Sn1–C2 | 93.6(2) | Br2–Sn2–C7 | 103.2(2) |
| O1–Sn1–C2 | 86.8(2) | Br1$^{i}$–Sn2–C7 | 83.6(2) |
| C1–Sn1–C2 | 119.1(4) | C6–Sn2–C7 | 115.3(3) |
| Br1–Sn1–C3 | 92.62(16) | Br2–Sn2–C8 | 101.4(2) |
| C1–Sn1–C3 | 114.9(3) | C7–Sn2–C8 | 114.8(3) |
| C2–Sn1–C3 | 124.5(3) | C6–Sn2–C8 | 120.0(3) |
| O1–Sn1–C3 | 80.70(18) | Br1$^{i}$–Sn2–C8 | 82.6(2) |
| P1–O1–Sn1 | 112.96(18) | | |
| P1–O1–Sn1–C3 | −7.1(3) | O1–Sn1–C3–C4 | 31.7(4) |
| Sn1–C3–C4–P1 | −47.5(5) | C3–C4–P1–O1 | 39.8(5) |
| C4–P1–O1–Sn1 | −14.7(3) | | |

H-bonds

| D–H–A | D–H (Å) | H–A (Å) | D–A (Å) | D–H–A (°) |
|---|---|---|---|---|
| C4–H4A–O1$^{ii}$ | 0.97 | 2.49 | 3.410(6) | 158 |
| C6–H6A–Br1$^{i}$ | 0.97 | 2.87 | 3.579(6) | 130 |

Symmetry operations: (i), $1-x,\ y-1/2,\ 1/2-z$; (ii), $x,\ 1/2-y,\ 1/2+z$.

Table 2
Comparison of selected geometric data about the chelated tin centres in solid **1**, **3**, **6** and **7**

| Compound | **1** (X = Cl)[a] | **3** (X = Cl)[b] | **6** (X = Cl)[c] | **1** (X = Br)[a] | **3** (X = Br)[d] | **1** (X = I)[a] | **1** (X = I)[a] | **7** (X = I)[d] |
|---|---|---|---|---|---|---|---|---|
| Temperature (K) | 301 | 301 | | 301 | 298 | 150 | 300 | 120 |
| Sn–X | 2.5119(7) | 2.536(3) | 2.560 | 2.6803(5) | 2.6918(8) | 2.9399(7) | 2.9363(4) | 3.0078(2) |
| X–Sn–O | 173.21(5) | 172.7(2) | 178.2 | 172.98(6) | 172.10(9) | 169.83(11) | 170.16(6) | 178.50(4) |
| Sn–O | 2.3971(17) | 2.352(5) | 2.292 | 2.379(2) | 2.354(3) | 2.373(4) | 2.386(2) | 2.2437(14) |
| C–Sn–O[e] | 79.60(8) | 80.2(3) | – | 80.00(11) | 80.70(18) | 81.1(2) | 81.00(12) | 90.71(7) |

[a] Ref. [6].
[b] Ref. [8].
[c] Ref. [7,9].
[d] This study.
[e] Chelate bite angle.

in the structure, see Fig. 3. As a consequence of the two $XMe_2SnCH_2CH_2$ groups on phosphorus having different roles molecules of solid **3** are chiral at P but the crystal structure is racemic due to the presence of equal amounts of both enantiomers as required by space group symmetry.

While **3** (X = Cl) [8] and **3** (X = Br) are isostructural, more detailed treatment of the X-ray data here for **3** (X = Br) has revealed the presence of weak intermolecular interactions not reported for **3** (X = Cl), which link the molecules into a supramolecular array. The primary chains, created by the bridging bromide, are reinforced by H-bonding interactions, C6–H6–Br1$^{i}$. Thus Br1 has two roles in the chain formation – as a H-bond acceptor and as an electron donor to Sn2, neither of which it fulfils particularly strongly. Other non-bonded interactions are C7–H7A–π, between a centrosymmetrically related pair of molecules, and C4–H4A–O1 H-bonds, see Figs. 4a and b. In Fig. 4b, the primary zig zag chains are viewed end on and it can be seen that the 'throw' (as in a crank-shaft), of the zig zag chains connects the molecules in a pair-wise manner in a direction parallel to the $(\bar{1},0,1)$ plane. The C4–H4A–O1 contacts, on the other hand, interconnect the chains in the direction of $c$ (the unit-cell edge). The overall effect is to create a double layer of molecules parallel to (1 0 0) and, because of the choice of origin for the structure determination, centred on $x = 1/2$. The interface between adjacent

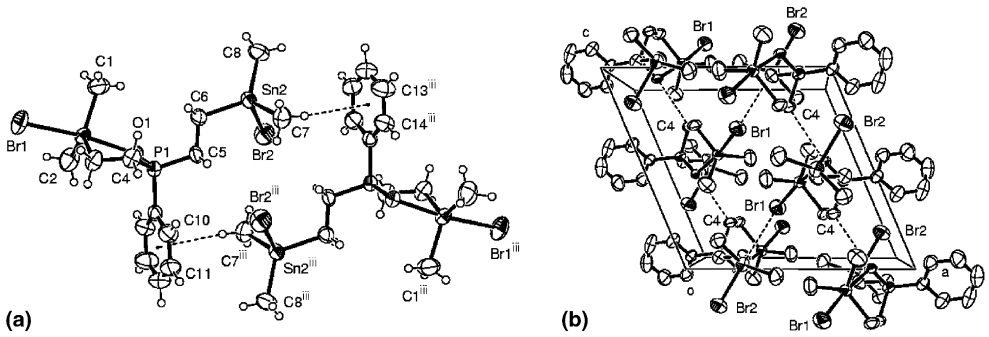


Fig. 4. (a) C–H–π interactions (dashed lines) between a centrosymmetrically related pair of molecules of **3** (X = Br). Symmetry operation (iii), $-x, -y, -z$; (b). A layer of molecules of **3** (X = Br). Selected atoms are labelled. Dashed lines represent (i) the Sn2–Br1 contacts evident in Fig. 3 or (ii) C4–H4A–O1 contacts given in Table 1 (H-bond type contacts).

double layers, at $x = 0$ and $x = 1$, is populated by Br2 atoms, phenyl groups and the C7 methyl group. This permits the C7–H7A–π interactions (Fig. 4a) to complete the 3-dimensional connectivity of the structure. With Cg representing the centroid (centre of gravity) of the phenyl ring, this interaction may be designated C7–H7A–π $^{iii}$ (symmetry operation: (iii), $-x, -y, -z$) and parameterised as H7A–Cg$^{iii}$ = 2.911, $H_{perp}$ (perpendicular distance of H from phenyl plane) = 2.898, C7–Cg$^{iii}$ 3.866 Å, C7–H7A–Cg$^{iii}$ = 172.99° and $\varphi = 5.47°$. The angle, $\varphi$, is the angle between the perpendicular from H(7A) to the plane and the vector H7A–Cg$^{iii}$.

### 2.3. Crystal structure of 7 (X = I)

Data were collected from a sample grown from EtOH solution. The atom labelling scheme for **7** (X = I) is indicated in Fig. 5a and selected geometric parameters are listed in Table 3. Comparisons with data for **1** (X = I) and other related compounds are shown in Table 2. The refinement of the structure indicated that a small amount of the diiodide, $I_2MeSnCH_2CH_2CH_2P(O)PhBu^t$ **8**, had co-crystallised with **7** (X = I). The additional iodide ligand (I2) simply replaces a methyl group (C1) in an equatorial site of the trigonal bipyramidal coordination of tin in **7** (X = I) but at a greater distance and these are the only atoms significantly affected by the replacement. Some selected geometric parameters for the diiodide are listed in Table 3, part b. However, as pointed out by Yoon and Parkin [14], bond length data for co-crystallised, disordered species, especially those for the minor component, can be seriously in error, when judged against values for pure compounds. The calculated separation of Sn1 and I2 of only 2.518(6) Å is completely unrealistic, when compared to the sum of the covalent radii for I and Sn, [2.73 Å]. A Sn–I bond length near 3 Å would be a reasonable value.

Compound **7** (X = I) exists as a chelated complex with an intramolecular Sn–O interaction. Thus, unlike for **1** (X = Cl, Br or I), crystallisation of **7** (X = I) from an alcohol solvent does not lead to a polymeric chain structure. Individual molecules of **7** (X = I) are chiral at phosphorus, but again the crystal structure is racemic due to the presence of both enantiomers in equal amounts as required by space group symmetry.

The six-membered chelate ring in **7** (X = I), with a chelate bite angle, C3–Sn1–O1, of 90.71(7)°, allows the formation of a more ideal trigonal bipyramidal geometry at tin, compared to the situations in **1**–**3**. This is shown by the $\tau$ parameter calculation, which indicated the geometry of **7** (X = I) has only a 5% distortion from trigonal bipyramidal towards square pyramidal [12].

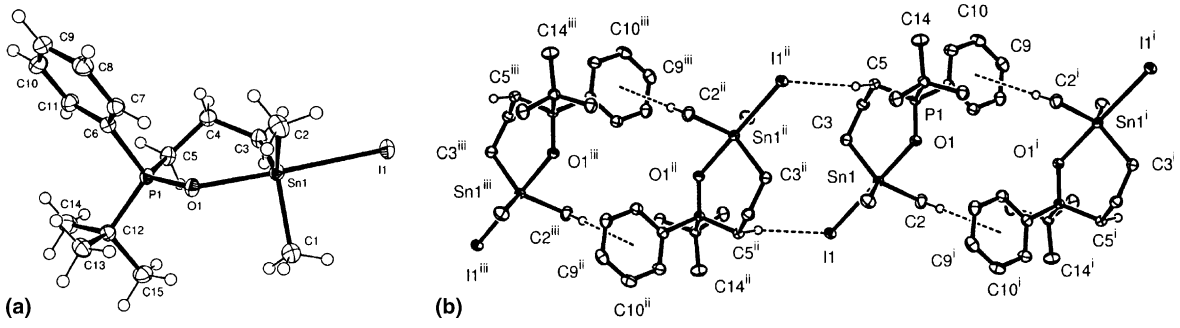


Fig. 5. (a) The molecule of **7** (X = I) showing the labelling scheme. (b) A portion of a double chain of molecules. Dashed lines represent C–H–I and C–H–π intermolecular interactions. H-atoms not involved in these interactions have been omitted for clarity and only selected atoms are labelled. Non-H atoms are shown as 50% probability ellipsoids and H atoms as spheres of arbitrary radius. Symmetry codes: (i), $-x, 1-y, 1-z$; (ii), $1-x, 1-y, -z$; (iii), $1+x, y, z-1$.

Table 3
Selected geometric parameters, (Å, °) for 7: (X = I)

| | | | | |
|---|---|---|---|---|
| I1–Sn1 | 3.0078(2) | Sn1–C1 | 2.139(4) | |
| Sn1–C2 | 2.131(2) | Sn1–C3 | 2.154(2) | |
| Sn1–O1 | 2.2437(14) | P1–O1 | 1.5216(14) | |
| C2–Sn1–C1 | 119.42(13) | C2–Sn1–C3 | 121.42(9) | |
| C1–Sn1–C3 | 119.11(12) | C2–Sn1–O1 | 87.62(7) | |
| C1–Sn1–O1 | 89.40(10) | C3–Sn1–O1 | 90.71(7) | |
| C2–Sn1–I1 | 91.38(6) | C1–Sn1–I1 | 92.07(10) | |
| C3–Sn1–I1 | 88.85(6) | O1–Sn1–I1 | 178.50(4) | |
| P1–O1–Sn1 | 131.67(8) | | | |
| P1–O1–Sn1–C3 | 1.36(13) | O1–Sn1–C3–C4 | 23.72(16) | |
| Sn1–C3–C4–C5 | −67.2(2) | C3–C4–C5–P1 | 79.2(2) | |
| C4–C5–P1–O1 | −45.37(17) | C5–P1–O1–Sn1 | 8.75(15) | |
| (b) Selected parameters for **8** | | | | |
| C2–Sn1–I2 | 117.65(18) | C1–Sn1–I2 | 2.1(2) | |
| C3–Sn1–I2 | 120.81(17) | O1–Sn1–I2 | 88.17(18) | |
| I2–Sn1–I1 | 93.29(17) | | | |
| H-bonds | | | | |
| D–H–A | D–H (Å) | H–A (Å) | D–A (Å) | D–H–A (°) |
| C5–H5A–I1$^{i}$ | 0.99 | 3.03 | 3.964(2) | 158 |

symmetry operation: (i), $1-x,\ 1-y,\ -z$.

Near ideal trigonal bipyramidal geometry was also found for the tin centre in **4**. The axial positions in **7** (X = I) are occupied by O1 and I1, with O1–Sn1–I1 = 178.50(4)°. The six-membered chelate ring has a conformation between half chair and envelope forms, the pucker parameters being, $Q = 0.588(2)$ Å, $\theta = 53.1(2)°$ and $\phi = 220.4(2)°$.

Molecules of **7** (X = I) are linked into double chains which are propagated perpendicular to $(10\bar{1})$, as a consequence of two intermolecular interactions: (i) a C5–H5A–I$^{i}$ interaction: symmetry operation: (i), $1-x,\ 1-y,\ -z$, and (ii) a C–H–π interaction with the phenyl ring, see Fig. 5b. Details of the C–H–π parameters are C–H = 0.99, H–Cg = 3.14, $H_{perp} = 2.77$ Å, C–H–Cg = 176.9 and $\gamma = 28.11°$, where Cg is the phenyl ring centroid, $H_{perp}$ the perpendicular distance of H from phenyl ring, and $\gamma$ the angle between H–Cg and $H_{perp}$. The distinct types of intermolecular interactions occur in centrosymmetrically related pairs (see Fig. 5b).

### 2.4. Comparison of acceptor strengths of 1, 4–7

The Sn–O bond lengths for the γ-stannylalkylphosphine oxides, $Cl_{3-n}Me_nSnCH_2CH_2CH_2P(O)Ph_2$ can be taken as measures of the acceptor strengths, the Lewis acidities, of the tin centres: the shorter the Sn–O bond length, the greater is the Lewis acidity of the tin centre. Thus the acceptor strengths increase in the sequence: **6** (X = Cl), i.e., $n = 2$ [7,9], **5**, i.e., $n = 1$ [3] and **4**, i.e., $n = 0$ [3], as the Sn–O bond lengths decrease in the sequence 2.292, 2.227(5) and 2.182(5) Å, respectively. While the exact details of the structure of **6** (X = Cl) are unknown and despite the structural differences between **4** and **5**, this sequence is as expected for a series of halo-organotin compounds, $Me_{3-n}RSnCl_n$. However, it is somewhat surprising that the tin centre in the di-halide **5** has a higher coordination number than that in the tri-halide **4**. The Sn–O bond lengths for **6** (X = Cl), 2.292 and **7** (X = I), 2.2437(14) Å suggest that the Lewis acidities for these γ-(halodimethylstannyl)alkylphosphine oxides are not too different, despite the differences in both the halo groups on tin and the organic groups on phosphorus: the lower temperature used for the data collection for **7** (X = I) [120 K, compared to the probable ambient temperature for **6** (X = Cl)] will result in a slight reduction of the Sn–O bond length.

Generally the formation of five-membered chelates is thermodynamically more favourable than that of six-membered chelates in tin complexes, as indicated, for example, by the formation of a five-membered rather than a six-membered chelate in methyl 5-deoxy-2,3-*O*-isopropylidene-5-*C*-[(iododiphenylstannyl)methyl]-α-D-lyxofuranoside [15]. However, comparisons of the Sn–O bond lengths in *chelate*-**1** (X = I) and **7** (X = I), and in *chelate*-**1** (X = Cl) and **6** (X = Cl), see Table 2, suggest stronger chelation in the γ-stannylalkylphosphine oxide derivatives. The reduced hindrance to the approach of the chelating site results in the apparent stronger chelation. As expected for trigonal bipyramidal geometries, as the axial Sn–O bond length decreases so the other axial bond length, Sn–X, increases.

### 2.5. Effects of the recrystallisation solvent on the solid-state structures of 3 and 7

The differences in the effects of the solvents used for recrystallisation of **1** were linked to the different H-bonding abilities of the solvents. From considerations of

the chelate effect [16,17], the chelate form of **1**, as obtained from non-hydroxylic solvents, would be the preferred structure [4]. However in alcohols, strong H-bonding between the HO group of the alcohol and the phosphine oxide oxygen atom becomes another very important stabilising influence. As the oxygen atom is more accessible in the open chain form than in the more hindered chelate form, the greater solvation of the chain form is considered sufficient to overcome the chelate effect in alcohol solutions. Thus, as a consequence of precursor structures being dominant, at least in alcohol solutions, the linear chain form of solid **1** is considered to be the most readily obtained from such solvents, at least for **1** (X = Cl, Br and I).

For all the ω-(stannylalkylphosphine) oxides, as with **1**, there will be a competition in alcohol solvents between H-bonding and chelation effects. For **1** (X = Cl, Br and I) as already described, this is won by H-bonding, but for **1** (X = NCS), the chelation effect is the dominant effect. That **1** (X = NCS) exhibits a different behaviour to **1** (X = halide) is probably linked to the fact that organotin isothiocyanates form stronger adducts than do the corresponding halides, as shown by formation constants [18].

As the same solid-state structure is obtained for **3**, on recrystallisation from alcohol and non-alcohol solvents, solvation effects of alcohol solvents cannot be the most significant factors for these compounds. For **3** in the solid state, only one of the tin centres is chelated, but in solution both are, see later, as shown by NMR spectra. As chelated structures are also obtained for **7** (X = I), even on recrystallisation from alcohol solvents, the chelation effect is dominant here too. The six-membered chelated structure of **7** (X = I) provides a less hindered oxygen centre than that in the five-membered chelate-**1**, with the consequence that H-bonding of the phosphine oxide oxygen with the alcohol solvent can proceed readily in the chelate. Thus, there is less difference in the solvation energies of potential chelate/open chain forms of both **3** and **7** compared to **1**, and so here the more stabilising chelate effect controls the structure obtained.

### 2.6. NMR spectra in solution

Reported chemical shift and coupling constant values obtained from multinuclear NMR [$^{1}$H, $^{13}$C, $^{31}$P and $^{119}$Sn] spectra for **1**, **2** and **6** clearly show that Sn–O interactions also occur in chloroform and methanol solution. This is interpreted to mean that on dissolution of **1**, **2** and **6**, structures closely related to the appropriate solid-state structures are produced including, for example, chelated structures as a result of the dissolution of either *chelate*-**1** or *polymer*-**1** in non alcohol solvents. The $^{1}$H NMR spectrum of **7** (X = I) [this study] and the multi-nuclear NMR spectra for **6** (X = F, Cl, Br and I) [7], in conjunction with IR spectra, indicate five coordinate tin species, with Sn–O interactions, as found in the solid state.

In contrast to the situations for **1**, **2**, **6** and **7**, solution NMR spectral data for **3** (X = Cl) in chloroform solutions led Weichmann and co-workers to propose a different solution structure to that determined in the solid state by X-ray crystallography. From the single $\delta^{119}$Sn value and the single $^{1}J(^{119}\mathrm{Sn}–^{31}\mathrm{P})$ value in the NMR spectra at room temperature and the $\nu$(PO) value in the IR spectrum in $CDCl_3$ solution, a symmetrical bicyclic structure with both tin atoms coordinated intramolecularly to the O atom, i.e., a bis-chelate structure as shown in Fig. 2 was proposed.

The $^{13}$C NMR spectra for **3** (X = Br or I), obtained in this study, indicated the equivalence of the two $Me_2SnCH_2CH_2$ fragments, as also reported by Weichmann and co-workers for **3** (X = Cl) [6]. As also found by Weichmann and co-workers, single $\delta^{119}$Sn value and single $^{1}J(^{119}\mathrm{Sn}–^{31}\mathrm{P})$ values are observed. However, no details of the $^{1}$H NMR spectrum of **3** (X = Cl) were, however, given [6]. As we found in this study, the $^{1}$H NMR spectra of **3** (X = Cl, Br and I) at room temperature in chloroform solution are complex for the Sn–$CH_2CH_2$–P fragments. The HSQC technique confirmed the direct H-C connectivities, the equivalence of the two Sn–$CH_2CH_2$–P fragments and the diastereomeric nature of each pair of methylene protons. For each of the four distinct protons in Sn–CHαHα′– CHβHβ′–P the signal was split into a dddd multiplet, due to couplings to four nuclei with spins of 1/2, see Table 4. As shown in Table 4, the $^{1}$H NMR spectra of **3**, specifically the high resolution (400 MHz) spectra of **3** (X = Br or I), are appreciably more complex than those of mono-cyclic **1**.

Use of the spin simulation module of the NUTS program [19] allowed reasonably good simulations of the $^{1}$H NMR spectra of the methylene protons to be obtained, see, for example, Fig. 6. Analysis indicated that two of the methylene protons are coupled to three H and one P nuclei, while the other two methylene hydrogens are coupled to two H and to two P nuclei, see Table 4. Such couplings, especially $J$(H,P), are difficult to account for by the simple monomeric structure for **3** (X = Cl) proposed by Weichmann et al. [8] and shown in Fig. 2. Dimeric structures, **3a**–**3c**, undergoing fast exchanges at room temperature, possibly with monomers, **3d**, as indicated in Scheme 1, would allow a more readily acceptable explanation for all the NMR data of **3** (X = Cl, Br and I). The equivalent species, **3a** and **3c**, having five-membered chelate rings, would undergo the least reorganisation among **3a**–**3d** to attain the solid-state structures. However, Weichmann et al. reported that **3** (X = Cl) was monomeric in chloroform solution, as determined by osmometry. It remains uncertain whether compounds **3** are monomeric at all concentrations. It is of course possible, even if improbable, that

Table 4
Selected NMR data[a] for compounds **1** and **3** in $CDCl_3$ solution at 27 °C

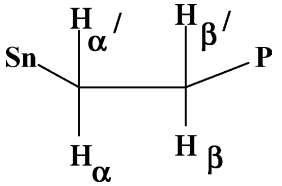


| Compound | δH($Me_2$ Sn) | δHα | | δHα′ | | δHβ | | δHβ′ | | δSn | δP |
|---|---|---|---|---|---|---|---|---|---|---|---|
| | [J(Sn,H)] | [*J*(H,H)] | [[*J*(H,P)]] | [*J*(H,H)] | [[*J*(H,P)]] | [*J*(H,H)] | [[*J*(H,P)]] | [*J*(H,H)] | [[*J*(H,P)]] | [*J*(Sn,P)] | |
| **3** (X = Cl) | 0.68 | 1.35 | | 1.58 | | 2.20 | | 2.36 | | 59.1 | |
| | [64.6, 60.9] | | | | | | | | | [62.3] | |
| | 0.67[b] | | | | | | | | | 60.5[b] | 58.0[b] |
| | 65.6[b] | | | | | | | | | [66.6][b] | |
| **3** (X = Br) | 0.80 | 1.26 | | 1.55 | | 2.18 | | 2.46 | | 44.7 | 58.6 |
| | [64.7, 62.0] | | | | | | | | | [64.7] | |
| | | [13.7] to Hα′ | [[4.8]] | [13.7] to Hα | [[31.1]] | [15.1] to Hβ′ | [[1.05]] | [15.1] to Hβ | [[4.1]] | | |
| | | [<0.5] to Hβ | [[20.0]] | [6.5] to Hβ | | [<0.5] to Hα | [[26.0]] | [6.2] to Hα | | | |
| | | [6.2] to Hβ′ | | [4.4] to Hβ′ | | [6.5] to Hα′ | | [4.4] to Hα′ | | | |
| **3** (X = I) | 0.94 | 1.33 | | 1.61 | | 2.21 | | 2.37 | | −0.7 | 58.0 |
| | [63.3, 60.6] | [13.3] to Hα′ | [[2.2]] | [13.3] to Hα | [[26.4]] | [15.1] to Hβ′ | [[ 1.4]] | [15.1] to Hβ | [[5.2]] | [67] | |
| | | [<0.5] to Hβ | [[20.1]] | [7.5] to Hβ | | [<0.5] to Hα | [[23.1]] | [7.5] to Hα | | | |
| | | [7.5] to Hβ′ | | [4.8] to Hβ′ | | [7.5] to Hα′ | | [4.8] to Hα′ | | | |
| **1** (X = Cl)[c] | 0.72 | 1.45 | | | | 2.61 | | | | 10.8 | 46.4 |
| | [69.4, 66.7] | [7.5] | [[20.2]] | | | [7.5] | [[8.9]] | | | [44.0] | |
| **1** (X = Br)[c] | 0.83 | 1.55 | | | | 2.61 | | | | −1.7 | 45.4 |
| | [69.1, 66.0] | [7.5] | [[19.8]] | | | [7.5] | [[9.2]] | | | [42.7] | |
| **1** (X = I)[c] | 1.00 | 1.68 | | | | 2.60 | | | | −31.8 | 45.9 |
| | [68.1, 65.3]] | [7.5] | [[20.1]] | | | [7.5] | [[8.9]] | | | [41.3] | |

[a] NMR frequencies as in Experimental section except for data from [8] and [6], where the frequencies in the order $^{1}H$, $^{119}Sn$ and $^{31}P$ were 200, 74.5 and 81 MHz and 400, 93.3 and 101.2 MHz, respectively.

[b] Ref. [8].

[c] δHα = δHα′ and δHβ = δHβ′ [6].

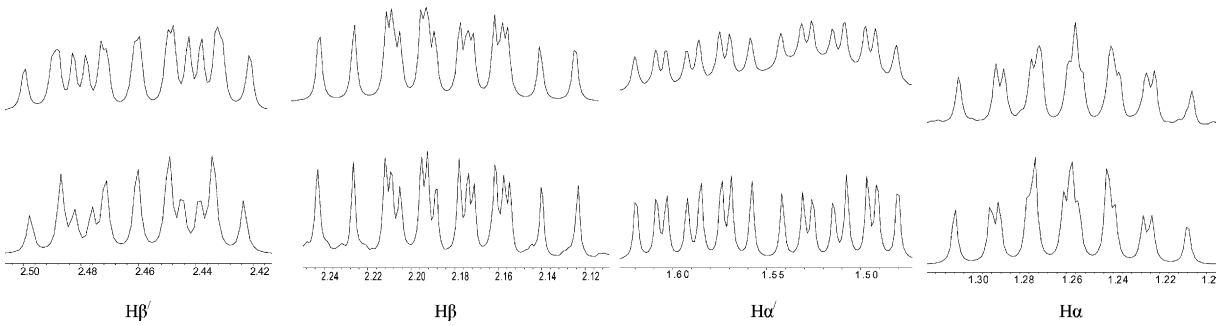


Fig. 6. The Sn–$CH_2CH_2$–P region in the $^1H$ NMR spectra of **3** (X = Br). Top row: actual spectra; bottom row: simulated spectra.

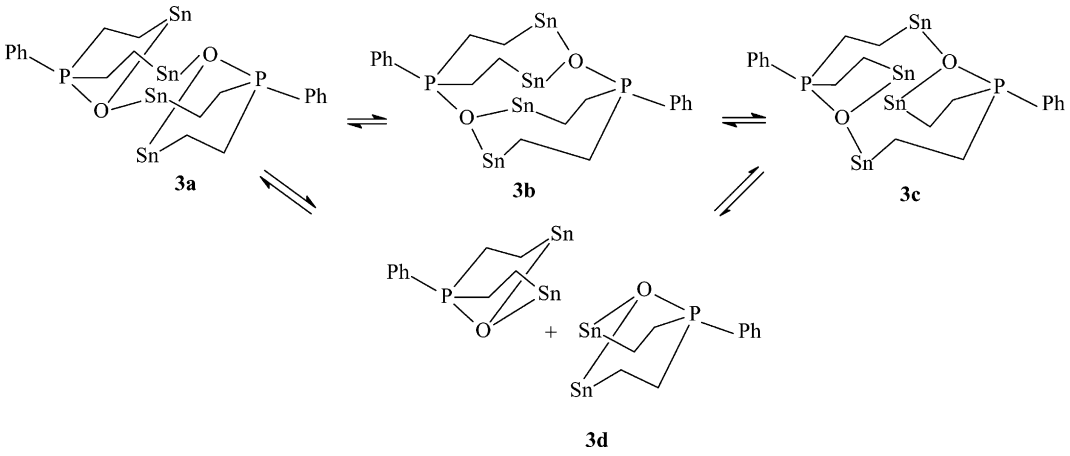


Scheme 1. Possible dimeric and monomeric structures for **3**, undergoing fast equilibrium exchanges at room temperature in solution. The $XMe_2$ substituents on the tin centres have been omitted for clarity.

dimeric forms dissociate, in $CHCl_3$ solutions, into two particles, which would give the same osmometric result as a monomeric species. Further work in this area is necessary to establish the structures in solution.

## 3. Experimental

### 3.1. General

Melting points were measured using a Kofler hot-stage microscope and are uncorrected. IR spectra were recorded on a Nicolet Magna-IR 760 instrument.

NMR spectra were obtained on Bruker 200 MHz, Bruker AC-250 250 MHz and Varian Unity Inova 400 MHz instruments. The NUTS program was utilised for the spectral simulations: parameters used were: frequency 400 MHz, spectral width 4000 Hz; offset 2000 Hz; points 8096; line width 1.0 Hz; $P_1 = 1000$ ppm; $P_2 = 1000$ ppm.

The compound, $Me_3SnCH_2CH_2CH_2PPhBu^t$ was obtained by a published procedure [10].

### 3.2. Synthesis

#### 3.2.1. 3 (X = Cl)

Bis[2-(chlorodimethylstannyl)ethyl]phenylphosphine oxide **3** (X = Cl) was a recrystallised sample, originally received as a gift from Dr. Weichmann, Halle.

$^1H$ NMR ($CDCl_3$, 200 MHz, 27 °C) $\delta$: 0.68 (s, 12H, $J(^{119,117}Sn–^1H) = 64.6$, 60.9 Hz, MeSn), 1.35 (m, 2H, $SnCH_2$), 1.58 (m, 2H, $CH_2Sn$), 2.20 (m, 2H, $CH_2P$), 2.36 (m, 2H, $CH_2P$), 7.2–7.6 (2m, 5H, aryl): [lit [4] values($CD_2Cl_2$, 30 °C): $\delta$: 0.67 (s, 12H, $J(^{119,117}Sn–^1H) = 65.6$ Hz, MeSn)].

$^{119}Sn$ ($CDCl_3$, 74.5 MHz, 27 °C) $\delta$: 59.1 $J(^{119}Sn–^{31}P = 62.3$ Hz): [lit. [4] value (toluene, 30 °C): $\delta$: 60.5 $J(^{119}Sn–^{31}P = 66.6$ Hz)].

#### 3.2.2. Bis(2-bromodimethylstannylethyl)phenylphosphine oxide 3 (X = Br)

This was obtained from **3** (X = Cl) (1 mmol) by halide exchange using excess NaBr (10 mmol) in $Me_2CO$ (50 ml). The reaction mixture, after leaving overnight with stirring, was rotary evaporated, the residue extracted

with $CHCl_3$, and recrystallised by slow evaporation of an ethanol solution: m.p. 157–158 °C.

Chem. anal. found: C, 26.3; H, 4.1. Calc. For $C_{14}H_{25}Br_2OPSn_2$: C, 26.4; H, 4.0%.

IR:(CsI, $cm^{-1}$) $\nu$ : 3060, 2999, 2968, 2918, 2899, 2814, 2782, 2362, 1708, 1651, 1590, 1483, 1437, 1417, 1399, 1313, 1270, 1220, 1185, 1136(PO), 1129, 1108, 1097, 1064, 1026, 846, 781, 742, 695, 659, 644, 594, 555, 543, 538, 524, 513, 496, 460, 436, 382, 335, 289, 280, 234, 210, 176.

$^1H$ NMR ($CDCl_3$, 400 MHz, 27 °C) $\delta$: 0.80 (s, 12H, $J(^{119,117}Sn–^1H) = 64.7$, 62.0 Hz, $Me_2Sn$), 1.26 (dddd, 2H, $J = 4.8, 6.2, 13.7, 20.0$ Hz, $SnCH_2$), 1.55 (dddd, 2H, $J = 4.4.6.5, 13.7, 31.1$ Hz, $CH_2Sn$), 2.18 (dddd, 2H, $J = 1.05, 6.5, 15.1, 26.0$ Hz, $CH_2P$), 2.46 (dddd,2H, $J = 4.1, 4.4, 6.2, 15.1$ Hz, $CH_2P$), 7.5-7.62 (m, 4H, o-+m-Ph), 7.62–7.7 (m, 1H, p-H).

$^{13}C$ NMR ($CDCl_3$, 100 MHz) $\delta$: 1.6, 10.1 $J(^{13}C–^{31}P = 5.5$ Hz), 25.4 $J(^{13}C–^{31}P = 65.4$ Hz), 127.1 $J(^{13}C–^{31}P = 91.9$ Hz), 129.7 $J(^{13}C–^{31}P = 11.7$ Hz), 130.4 $J(^{13}C–^{31}P = 9.6$ Hz), 133.5 $J(^{13}C–^{31}P = 2.8$ Hz). [$J(^{13}C–^{119,117}Sn)$ values were not detected].

$^{31}P$ NMR ($CDCl_3$, 101.2 MHz) $\delta$: 58.6.

$^{119}Sn$ NMR ($CDCl_3$, 93.3 MHz) $\delta$: 44.7 $J(^{119}Sn–^{31}P = 64.7$ Hz).

### 3.2.3. Bis[2-(iododimethylstannyl)ethyl]phenylphosphine oxide **3** (X = I)

Compound **3** (X = I), was similarly obtained from **3** (X = Cl), by halogen exchange, using NaI.

Chem. anal. found: C, 23.1; H, 3.3. Calc. For $C_{14}H_{25}I_2OPSn_2$: C, 23.0; H, 3.4%.

$^1H$ NMR ($CDCl_3$, 400 MHz, 27 °C) $\delta$: 0.94 (s, 12H, $J(^{119,117}Sn–^1H) = 63.3$, 60.6 Hz, MeSn), 1.33 (dddd, 2H, $J = 2.2, 7.5, 13.3, 20.1$ Hz, $SnCH_2$), 1.61 (dddd, 2H, $J = 4.8, 7.5, 13.3, 26.4$ Hz, $CH_2Sn$), 2.21 (dddd, 2H, $J = 1.4, 7.5, 15.1, 23.1$ Hz, $CH_2P$), 2.37 (dddd, 2H, $J = 5.2, 4.8, 7.5, 15.1$ Hz, $CH_2P$), 7.6(m, 5H, aryl).

$^{31}P$ NMR ($CDCl_3$, 101.2 MHz) $\delta$: 58.0.

$^{119}Sn$ ($CDCl_3$, 93.3 MHz) $\delta$: −0.7 $J(^{119}Sn–^{31}P = 67$Hz).

### 3.2.4. t-Butyl[3-(iododimethylstannyl)propyl]phenylphosphine oxide **7** (X = I)

Solutions of $Me_3SnCH_2CH_2CH_2PPhBu^t$ [10] (0.1 mmol) in methanol (15 ml) and $I_2$ (0.1 mmol) in methanol (50 ml) were mixed and left at room temperature with access to air until the reaction mixture became colourless. Removal of all volatiles under vacuum left a residue, which was recrystallised from EtOH.

Chem. anal. found: C, 35.9; H, 5.2. Calc. For $C_{15}H_{26}IOPSn$: C, 36.1; H, 5.3%.

$^1H$ NMR ($CDCl_3$, 200 MHz) $\delta$: 0.98 (s, 6H, Me-Sn), 1.08 (dd, 9H, $J_{H,H} = 6.4$Hz, $J_{P,H} = 21.4$ Hz $CMe_3$), 1.76 (t, 2H, $CH_2Sn$), 2.09 (m, 2H,$CH_2CH_2CH_2$), 2.26 (t, 2H, $CH_2P$), 7.61 (m, 5H, Ph).

$^{13}C$ NMR ($CDCl_3$, 50 MHz) $\delta$: 6.1 [$Me_2Sn$], 20.4 [$J(^{13}C–^{31}P) = 5.5$ Hz, $CH_2CH_2Sn$], 22.6 [$J(^{13}C–^{31}P) = 10.9$ Hz, $CMe_3$], 23.9[$CMe_3$], 26.3[$CH_2Sn$], 33.1[$J(^{13}C–^{31}P) = 67.4$Hz, $CH_2P$)], 126.5[$J(^{13}C–^{31}P) = 89$ Hz, $C_i$], 129.0 [$J(^{13}C–^{31}P) = 11.0$ Hz,$C_m$], 131.8 [$J(^{13}C–^{31}P)$ 8.3 Hz, $C_o$], 133.0 [$J(^{13}C–^{31}P) = 3$ Hz].

## 3.3. Crystallography

### 3.3.1. Data collection

Intensity data for **3** (X = Br) were obtained at 298(2) K with a Bruker SMART 1000 CCD area detector diffractometer controlled by SMART software [20]. Cell refinement and data reduction were carried out with the program SAINT [20]. SADABS [20] was used to apply correction for absorption by the multi-scan method, i.e., in a semi-empirical manner based on the comparison of the intensities of equivalent reflections. For **7** (X = I) intensity data were collected at 120(2) K on the Enraf Nonius KappaCCD area detector diffractometer with an Enraf Nonius FR591 rotating anode X-ray source at the EPSRC's crystallographic service at Southampton. The unit cell was determined and the data collected using the programs DENZO [21] and COLLECT [22]. The data were corrected for absorption by means of the program SORTAV [23,24].

### 3.3.2. Structure solution and refinement

For both structures the direct methods approach of SHELXS 97 [25] was used to solve the structure and refinement was by means of SHELXS 97 [26]. All non-H atoms were refined anisotropically. H-atoms were placed in calculated positions and refined with a riding model. ORTEP [27] was used in the preparation of the Figures and SHELXS 97 and PLATON [28] in the preparation of the tables. Data collection and refinement details are listed in Table 5.

In the final stages of the refinement of **7** (X = I) the model was extended to include the replacement of the C1 methyl group by further iodine, I2, corresponding to inclusion in the sample crystal of 3.72(10)% of the diiodo compound, $I_2MeSnCH_2CH_2CH_2P(O)PhBu^t$ **8**. The low occupancy of I2 and its close proximity to C1 resulted in a very low and unrealistic estimate of the Sn(1)–I(2) bond length [2.518(6) Å] and accordingly I2 has been ignored in the preparation of Fig. 5 presented here.

## 4. Supplementary material

Crystallographic data for the structural analyses have been deposited with the Cambridge Crystallographic Data Centre, CCDC numbers 180247 and 210439 for compounds **3** (X = Br) and **7** (X = I), respectively. Copies of this information may be obtained from the

Table 5
Crystal data and structure refinement

| Compound | **3** (X = Br) | **7** (X = I) |
|---|---|---|
| Empirical formula | $C_{14}H_{25}Br_2OPSn_2$ | $C_{15}H_{26}IOPSn$ |
| Formula weight | 637.51 | 498.92 |
| Temperature (K) | 298(2) | 120(2) |
| Wavelength (Å) | 0.71073 | 0.71073 |
| Crystal system | monoclinic | triclinic |
| Space group | $P2_1/c$ | $P\bar{1}$ |
| Unit cell dimensions | | |
| $a$ (Å) | 12.2894(6) | 7.9651(4) |
| $b$ (Å) | 16.5951(7) | 9.8291(5) |
| $c$ (Å) | 11.6599(5) | 12.6926(6) |
| $\alpha$ (°) | 90 | 75.2350(16) |
| $\beta$ (°) | 113.1420(10) | 79.9980(17) |
| $\gamma$ (°) | 90 | 82.0080(16) |
| Volume (Å$^3$) | 2186.62(17) | 941.59(8) |
| $Z$, $D_{calc}$ (Mg m$^{-3}$) | 4, 1.937 | 2, 1.760 |
| Absorption coefficient (mm$^{-1}$) | 6.007 | 3.074 |
| $F(000)$ | 1208 | 484 |
| Crystal colour, size (mm) | colourless, $0.36 \times 0.24 \times 0.17$ | colourless, $0.30 \times 0.20 \times 0.15$ |
| $\theta$ range for data collection (°) | 1.80–25.05 | 2.15–28.98 |
| Index ranges | $-12 \leqslant h \leqslant 14$ | $-10 \leqslant h \leqslant 10$ |
| | $-19 \leqslant k \leqslant 17$ | $-13 \leqslant k \leqslant 13$ |
| | $-13 \leqslant l \leqslant 13$ | $-16 \leqslant l \leqslant 17$ |
| Reflections collected/unique | 12,902/3843 [$R_{int} = 0.0290$] | 8822/4371 [$R_{int} = 0.0133$] |
| Completeness (%) to $\theta$ limit (°) | 95.8 (to 25.05) | 99.3 (to 25.00) |
| Absorption correction | semi-empirical from equivalents | semi-empirical from equivalents |
| Max. and min. transmission | 0.928 and 0.650 | 0.6556 and 0.4591 |
| Refinement method | full-matrix least squares on $F^2$ | full-matrix least squares on $F^2$ |
| Data/restraints/parameters | 3843/0/185 | 4371/0/185 |
| Goodness-of-fit on $F^2$ | 1.060 | 1.080 |
| Final $R$ indices [$I > 2\sigma(I)$] | $R_1 = 0.0348$, $wR_2 = 0.0897$ | $R_1 = 0.0188$, $wR_2 = 0.0458$ |
| $R$ indices (all data) | $R_1 = 0.0479$, $wR_2 = 0.0942$ | $R_1 = 0.0211$, $wR_2 = 0.0467$ |
| Largest differential peak and hole (e Å$^{-3}$) | 0.655 and −1.108 | 0.713 and −0.674 |

Director, CCDC, 12 Union Road, Cambridge CB2 1EZ, UK (fax: + 44-1223-336033; e-mail: deposit@ccdc.cam.ac.uk).

## Acknowledgements

The authors thank the EPSRC for the use of both the X-ray service at the University of Southampton, for data collection, and the Chemical Database service at Daresbury. SMSVW and JLW thank CNPq (Brazil) for financial support.

## References

[1] H. Weichmann, C. Mugge, A. Grand, J.B. Robert, J. Organomet. Chem. 238 (1982) 343, and references therein.
[2] H. Weichmann, C.G. Quell, A. Tzschach, Z. Anorg. Allg. Chem. 462 (1980) 7.
[3] M. Seibert, K. Merzweiler, C. Wagner, H. Weichmann, J. Organomet. Chem. 650 (2002) 25.
[4] T.N. Mitchell, B. Godry, J. Organomet. Chem. 490 (1995) 45.
[5] H. Preut, B. Godry, T.N. Mitchell, Acta Crystallogr., Sect. C C48 (1992) 1894.
[6] W.T.A. Harrison, R.A. Howie, C.M. Munro, J.L. Wardell, J. Chem Soc., Dalton Trans. (2001) 2593.
[7] T.N. Mitchell, B. Godry, J. Organomet. Chem. 516 (1996) 133.
[8] M. Dargatz, H. Hartung, E. Kleinpeter, B. Rensch, D. Schollmeyer, H. Weichmann, J. Organomet. Chem. 361 (1989) 43.
[9] H. Preut, B. Godry, T.N. Mitchell, reported to be in press in Ref. 7.
[10] H. Weichmann, J. Meunier-Piret, J. Organomet. Chem. 309 (1986) 267.
[11] J.E. Huheey, E.A. Keiter, R.L. Keiter, Inorganic Chemistry, Principles of Structure and Reactivity, fourth ed., Harper Collins, New York, 1993.
[12] A.W. Addison, T.N. Rao, J. Reedijk, J. van Rijn, G.C. Verschoor, J. Chem. Soc., Dalton Trans. (1984) 1349.
[13] D. Cremer, J.A. Pople, J. Am. Chem. Soc. 97 (1975) 1354.
[14] K. Yoon, G. Parkin, Inorg. Chem. 31 (1992) 1656.
[15] C.C.C. Chibesakunda, P.J. Cox, H. Rufino, J.L. Wardell, Acta Crystallogr., Sect. C C54 (1998) 925.
[16] J.J.R.F. da Silva, J. Chem. Ed. 60 (1963) 390.
[17] W.P. Jencks, Proc. Natl. Acad. Sci. USA 78 (1981) 4046.
[18] J.L. Wardell, J. Chem. Soc. A (1971) 2628.
[19] NUTS: 2D, Version 4.95, Acorn NMR, 1995.
[20] SADABS, SMART and SAINT, Bruker AXS Inc., Madison, WI.

[21] Z. Otwinowski, W. Minor, Macromolecular crystallography, Part A, in: C.W. Carter, R.M. Sweet (Eds.), Methods in Enzymology, vol. 276, Academic Press, New York, 1997, p. 307.
[22] R. Hooft, COLLECT, Nonius BV, Delft, The Netherlands, 1998.
[23] R.H. Blessing, Acta Crystallogr., Sect A A51 (1995) 33.
[24] R.H. Blessing, J. Appl. Crystallogr. 30 (1997) 421.
[25] G.M. Sheldrick, Acta Crystrallogr., Sect. A A46 (1990) 467.
[26] G.M. Sheldrick, SHELXS 97. Program for Crystal Structure Refinement, University of Göttingen, Germany, 1997.
[27] L.J. Farrugia, J. Appl. Crystrallogr. 30 (1997) 565.
[28] A.L. Spek, J. Appl. Crystallogr. 36 (2003) 7.